

This work was written as part of one of the author's official duties as an Employee of the United States Government and is therefore a work of the United States Government. In accordance with 17 U.S.C. 105, no copyright protection is available for such works under U.S. Law.

Public Domain Mark 1.0

<https://creativecommons.org/publicdomain/mark/1.0/>

Access to this work was provided by the University of Maryland, Baltimore County (UMBC) ScholarWorks@UMBC digital repository on the Maryland Shared Open Access (MD-SOAR) platform.

**Please provide feedback**

Please support the ScholarWorks@UMBC repository by emailing [scholarworks-group@umbc.edu](mailto:scholarworks-group@umbc.edu) and telling us what having access to this work means to you and why it's important to you. Thank you.



# Intermittency in the Magnetic Hump in the VLISM

L. F. Burlaga<sup>1</sup>, D. B. Berdichevsky<sup>2,3</sup>, L. K. Jian<sup>4</sup>, J. Park<sup>5</sup>, A. Szabo<sup>4</sup>, and N. F. Ness<sup>6</sup><sup>1</sup>Leonard F. Burlaga, Inc., Davidsonville, MD 21035, USA<sup>2</sup>IFIR/UNR-CONICET, Esmeralda y 27 de Febrero, Rosario, Santa Fe, Argentina<sup>3</sup>Aleyon Technical Services, JV, LLC, USA<sup>4</sup>Heliophysics Science Division, NASA/GSFC, Greenbelt, MD 20771, USA<sup>5</sup>University of Maryland, Baltimore County, Baltimore, MD 21250, USA<sup>6</sup>Independent Scholar, Landenberg, PA 19350-9350, USA

Received 2023 September 28; revised 2023 November 30; accepted 2023 December 11; published 2024 March 13

## Abstract

Voyager 1 has been moving through the very local interstellar medium (VLISM) for  $\sim 1$  solar cycle, from 122.58 au on 2012/DOY 238 (August 25) to 158.5 au on 2023.0. A magnetic hump was observed, beginning with an abrupt increase (jump) in the magnetic field strength  $B$  and proton density  $N$  by a factor of 1.35 and 1.36, respectively, in the course of  $\sim 8$  days, ending at  $\sim 2020$ /DOY 147, after which it remained above the pre-jump levels for 2.6 yr, and it is still increasing. Unlike the three previous jumps, which were followed by a slow decrease in  $B$ ,  $B$  in the magnetic hump continued to increase to a maximum value  $\sim 0.56$  nT at  $\sim 2021$ /DOY 146.7. This paper discusses the intermittency of the magnetic field components and strength in the magnetic hump, and compares them with previous values in the VLISM. We consider the intermittency of the increments of  $\mathbf{B}$  and its components observed on a scale of one day. The distribution function (the Tsallis distribution or  $q$ -distribution function) of the increments of hourly averages of the components of  $\mathbf{B}$  had a Gaussian core associated with randomness in the observations, and it had two symmetric tails associated with the observed intermittency. The parameters  $q$ -dBR1,  $q$ -dBT1, and  $q$ -dBN1 increased slightly to a broad maximum with  $q = \sim 1.4$  between 2018 and 2019, and then decreased to  $q \sim 1$  (corresponding to no intermittency) in 2022. The  $Z$ -component of the magnetic field is within  $4 \pm 4$  counts ( $0.02$  nT  $\pm 0.02$  nT).

Unified Astronomy Thesaurus concepts: [Interstellar medium](#) (847)

## 1. Introduction

General overviews of the interaction between the heliosphere and the interstellar medium as well as the heliopause, which separates these two regions, were published by Holzer (1989), Parker (1963), and Kleimann et al. (2022). Voyager 1 (V1) was launched in 1977 and has been making observations during the last 45 yr, for more than four solar cycles, out to at least 160 au. The spacecraft moved through the heliosphere, across the termination shock, through the heliosheath, across the heliopause on 2012 August 25, and it has been moving through the interstellar medium for the last  $\sim 11$  yr, which is nearly one solar cycle (Burlaga et al. 2013; Krimigis et al. 2013; Gurnett et al. 2013; Stone et al. 2013). The heliopause is the boundary of the heliosphere (Parker 1963; Pogorelov et al. 2017) between the hot ( $10^5$ – $10^6$  K; Livadiotis et al. 2011) plasma flowing outward from the Sun and the relatively cold ( $10^4$  K) plasma in the very local interstellar medium (VLISM; Zank 2015). The Voyager 2 spacecraft also moved through the heliosphere, across the termination shock, through the heliosheath, and across the heliopause (Burlaga et al. 2013; Gurnett et al. 2013; Stone et al. 2013 and Krimigis et al. 2013), but we do not discuss these results in the present paper.

It has been shown that the Sun itself might be responsible for magnetohydrodynamic (MHD) processes that produce the magnetic hump that was observed recently in the VLISM (Burlaga et al. 2023). Burlaga et al. (2020b) observed

intermittency in the VLISM. There is no unique definition of intermittency (Frisch 1995). For a one-dimensional signal in the solar wind, heliosheath, and VLISM, it is customary to describe intermittency by the nonextensive parameter,  $q$ , associated with the Tsallis distribution function (Tsallis 1988), also called the  $q$ -distribution function for a medium that is not in statistical equilibrium. This distribution is given by the  $q$ -distribution function,  $A[1 + (q - 1)\beta x^2]^{1/(q-1)}$ , where  $q$  is the nonextensive parameter, and the variable  $x$  is an increment of a magnetic field component,  $x = \text{dBR1}$ ,  $\text{dBT1}$ , and  $\text{dBN1}$  for the 1 hr increments of BR, BT, and BN, respectively, as discussed in the following section. Tsallis statistics are applicable to systems that are out of equilibrium and have strong correlations. Tsallis statistics are related to Boltzman-Gibbs statistics via the standard map (Tirnakli & Borges 2016).

This paper (1) discusses the intermittency of the components of the magnetic field  $\mathbf{B}$  in the magnetic hump and (2) compares these results with earlier measurements of intermittency in the VLISM. It is shown that the intermittency in the magnetic hump differs significantly from that in the earlier observations or Voyager 1 of  $\mathbf{B}$  and the VLISM. The instrument and methods for processing the data observed by the magnetometer on Voyager 1 are described by Behannon et al. (1977) and Berdichevsky (2009, 2015).

A plot of the magnetic hump based on one-hour averages of  $B$  is shown in Figure 1, which is the same as was discussed by Burlaga et al. (2023). The magnetic hump began with an abrupt jump in the magnitude of  $\mathbf{B}$ , ending near 2020/DOY 146, which was labeled pf2 by Burlaga et al. (2020a), who showed that  $B_2/B_1 = 0.46$  nT/0.34 nT = 1.35. This jump was accompanied by a similar jump in the density,  $N_2/N_1 = 1.36$ .



Original content from this work may be used under the terms of the [Creative Commons Attribution 4.0 licence](#). Any further distribution of this work must maintain attribution to the author(s) and the title of the work, journal citation and DOI.

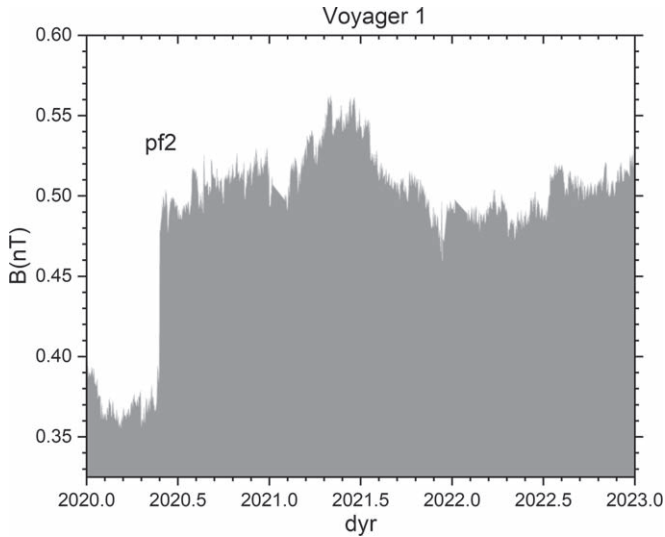


**Figure 1.** The magnetic hump. Note the jump, pf2 at the arrival of the magnetic hump at Voyager 1, the  $B$  peak in  $B$  between  $\sim 2021.1$  and  $\sim 2022.0$ , and the increasing  $B$  near the end of the plot.

Unlike the shocks sh1 and sh2 and a pressure front that were observed earlier in the VLISM by Voyager 1 (Burlaga et al. 2020a), which were followed by a slow decrease in  $B$ , Figure 1 shows that  $B$  increased for nearly a year after encountering the jump pf2.

Like the pressure front pf1, pf2 was not accompanied by intense electron plasma oscillations, enhanced turbulence activity (Fraternali et al. 2020), or increased energetic particle intensities (S.M. Krimigis 2021, private communication; J. Rankin 2022, private communication), which suggests that the jump in  $B$  at the magnetic hump near day 2020/146.90 was not a shock, even though the passage time of pf2 was shorter than 8 days. The two shocks observed by Voyager 1 in the VLISM had passage times of 5.4 and 3.3 days.

Figure 1 shows that beyond pf2, the magnetic field increased to a maximum of  $\sim 0.56$  nT at approximately 2021/DOY 146, in contrast to the decreases following the abrupt changes sh1, sh2, and pf1. The magnetic field following the maximum in the hump decreased to 0.47 nT, but it did not return to the pre-jump value of  $\sim 0.36$  nT. Instead,  $B$  increased erratically to 0.52 nT at the end of the data set at the end of 2022. Thus, the magnetic hump is a very large structure with strong magnetic fields, which was not seen in the VLISM before. Burlaga et al. (2023) presented evidence that this magnetic hump was produced by the Sun during the declining phase of the solar cycle.

Close inspection of Figure 1 shows that  $B$  fluctuated significantly at small scales throughout the magnetic hump. Burlaga et al. (2023) noted that that some of these fluctuations, observed from  $\sim 2021.2$  to 2021.5, appear to be quasi-periodic, with a period close to but somewhat longer than the solar rotation period. The other fluctuations in Figure 1 are a combination of noise and intermittent spikes of the magnetic field. The purpose of this paper is to determine the intermittency of these fluctuations and compare it with the intermittency observed in the VLISM prior to the arrival of the magnetic hump at Voyager 1.

## 2. Measurements of the Intermittency of the Magnetic Field in the Magnetic Hump and Earlier Observations of the VLISM

Intermittency refers to the relatively large spikes that are observed in a time series of measurements. There is no unique definition of intermittency (Frisch 1995). For a one-dimensional signal or a single component of a vector field  $\mathbf{B}$ , it is customary to define intermittency in terms of a set increments  $dX(t, \tau_m) \equiv X(t + \tau_m) - X(t)$ , where  $t$  is the observation time, and  $X$  is a component of  $\mathbf{B}$  or the magnitude of  $\mathbf{B}$ . Intermittency is seen as non-Gaussian spikes of  $dX(t)$ . The significance of these spikes is that they are large enough to measure accurately, whereas the smaller-amplitude fluctuations are often contaminated or obscured by noise.

Associated with the time series of the increments  $dX(t, \tau_m)$  is the distribution function of these increments. Burlaga et al. (2020b) showed that the distribution function of increments of the components of  $\mathbf{B}$  in the magnetic hump during 2015 through 2019 was non-Gaussian. We discuss the distribution function of the increments of the components of  $\mathbf{B}$  in the magnetic hump during 2020 through 2022.

A  $q$ -Gaussian distribution function can be used to describe the distribution of increments of the components of the magnetic field in the VLISM. The  $q$ -Gaussian distribution was introduced by Tsallis (1988, 2004) in his development of a nonextensive statistical mechanics. The relevance of the  $q$ -Gaussian distribution of the solar wind, heliosheath, and VLISM has been demonstrated by Burlaga et al. (2006).

The  $q$ -Gaussian distribution is introduced above. The core of the distribution is a Gaussian distribution, and the tail of the distribution is related to  $q$ , which determines the intermittency of the fluctuations of the components of  $\mathbf{B}$  and determines the size of the tails of the distribution. For a Gaussian distribution,  $q = 1$  indicates no intermittency and no non-Gaussian distribution. For a non-Gaussian,  $q = 7$  indicates very high intermittency (large tails). The  $q$ -Gaussian distribution appears in the magnetic field fluctuations over a range of scales in the solar wind, the heliosheath, and the VLISM (e.g., Burlaga et al. 2006; Sorriso-Valvo et al. 1999).

The measurements of  $\mathbf{B}$  are made in a coordinate system that is fixed on the spacecraft, the spacecraft-centered RTN coordinate system. In this system, the dimensionless unit vector  $\mathbf{R}$  is directed radially away from the Sun to the spacecraft,  $\mathbf{T}$  is parallel to the solar equatorial plane and aligned with the direction of the Sun's rotation, and the unit vector  $\mathbf{N}$  completes the right-handed coordinate system. Thus,  $\mathbf{B} = B_R \mathbf{R} + B_T \mathbf{T} + B_N \mathbf{N}$ . Note that the  $\mathbf{T}$  direction is only  $\sim 30^\circ$  from the average magnetic field direction, and the unit vectors  $\mathbf{N}$  and  $\mathbf{R}$  are nearly normal to the average magnetic field throughout the interval considered. Thus, the fluctuations of  $B$  near the average magnetic field direction are primarily Alfvénic fluctuations, which are incompressible fluctuations, and variations in the  $\mathbf{R}$  and  $\mathbf{N}$  directions are transverse fluctuations. The V1 spacecraft is not rotating, except for calibrations and special circumstances, and it is oriented such that the antenna is directed toward the Earth. Thus, one component of each of the two magnetometers (outboard and inboard) is oriented close to in the  $\mathbf{R}$  direction at large distances from the Sun. Since the  $\mathbf{R}$  direction is nearly normal to the average magnetic field direction in general, the magnetic field component in the  $\mathbf{R}$  direction is generally weak.

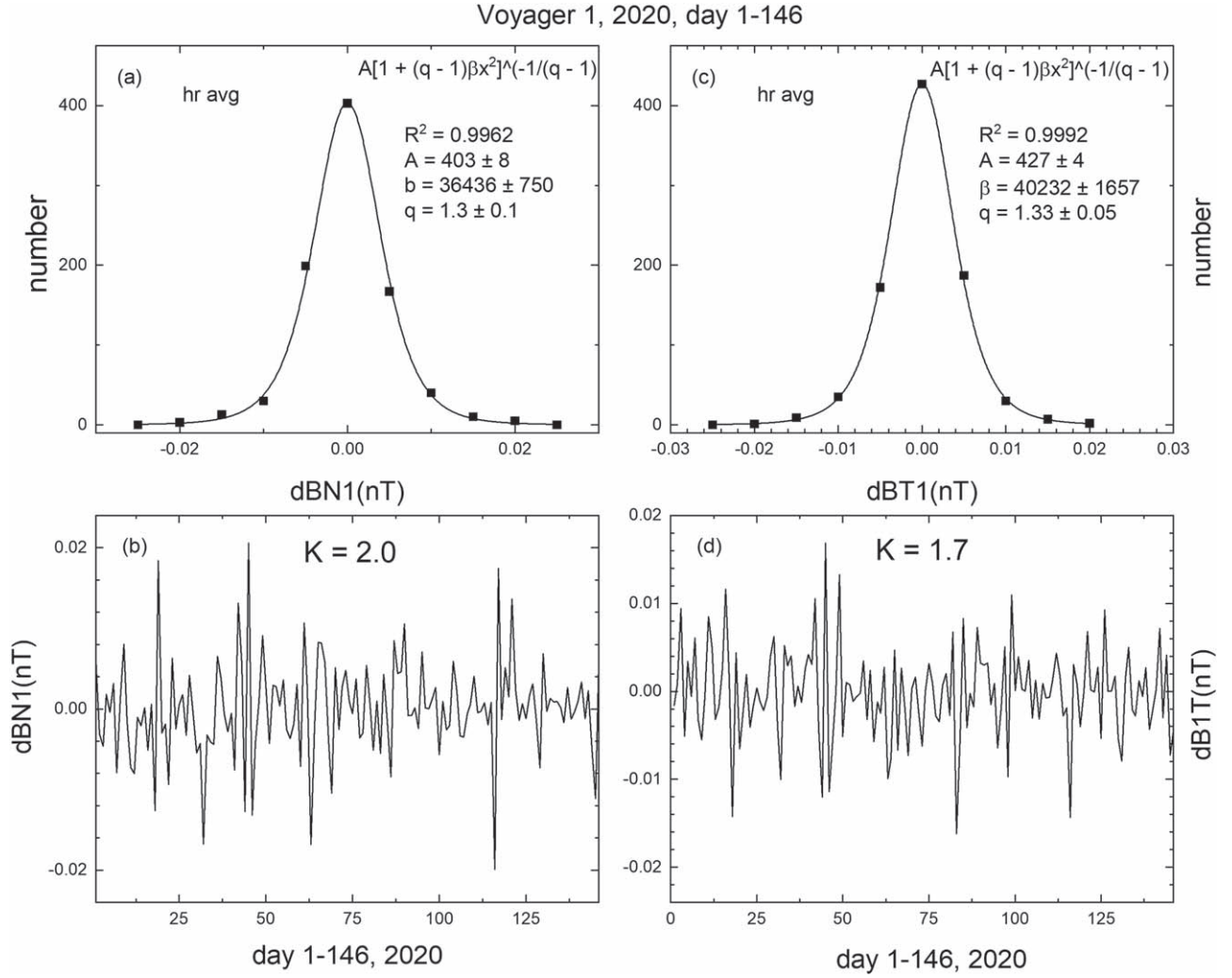


**Figure 2.** Intermittency in the dBN1 and the dBT1 components observed just before the magnetic hump in 2020.

The increments in BN beyond  $\sim 5$  au are primarily transverse to the average magnetic field, and the increments in BT are primarily longitudinal (compressible) as far as 146 au at Voyager 1. The dominant transverse component is related to Alfvén waves, and the compressible component is related to magnetosonic waves.

Our aim in this paper is to identify and measure tails in the fluctuations of the components  $dBN(t)$ ,  $dBT(t)$ , and to some extent  $dBR(t)$ , in the magnetic hump observations in the spacecraft-centered RTN coordinate system, using the non-extensive parameter  $q$  of the  $q$ -distribution function defined above. The integer 1 in  $dBN1(t)$  etc. means that we are dealing with 1 hr observations. We also compare the magnetic hump observations of  $\mathbf{B}$  with previous observations of the magnetic field in the VLISM.

### 3. Distribution of Increments of the Components in the Magnetic Field in the Magnetic Hump

As an introduction to the plots that describe intermittency in the VLISM, we begin the discussion of intermittency in the observations of hourly averages of the BN and BT components of the interstellar magnetic field using the data in 2020 just

ahead of the jump pf2 and the magnetic hump, from day 1 to 146, 2020, which are shown in Figure 2. The lower left panel in Figure 2(b) shows the time series of successive hourly increments of  $dBN1(t, tm) = dBN1(t + tm) - dBN1(t)$  where  $\tau_m = 1$  hr. The time series appears to be continuous, but that is because we connect points between data-gap point when drawing the plot. In fact, there are significant data gaps each day, some small and some large, but we consider only segments with two or more consecutive hourly averages when calculating the hourly increments of dBN1 and dBT1. It is possible to study the increments over a range of timescales, but we restrict the analysis to the one-hour increments. These increments suffice to compute the distribution function of the increments dBN1 from day 1 to day 146, as plotted in Figure 2(a).

The final step is to fit the observed distribution of increments with the  $q$ -distribution function, which gives the curve plotted in Figure 2(a). The  $q$ -distribution provides an excellent fit to the distribution of increments, with  $R^2 = 0.996$ , which justifies our use of the  $q$ -distribution function to describe observations of the increments of the field,  $dBN1(t)$ . The maximum amplitude of the distribution is given by  $A = 403 \pm 8$ . The parameter  $\beta = 36,036 \pm 750$  measures the core of the distribution. The



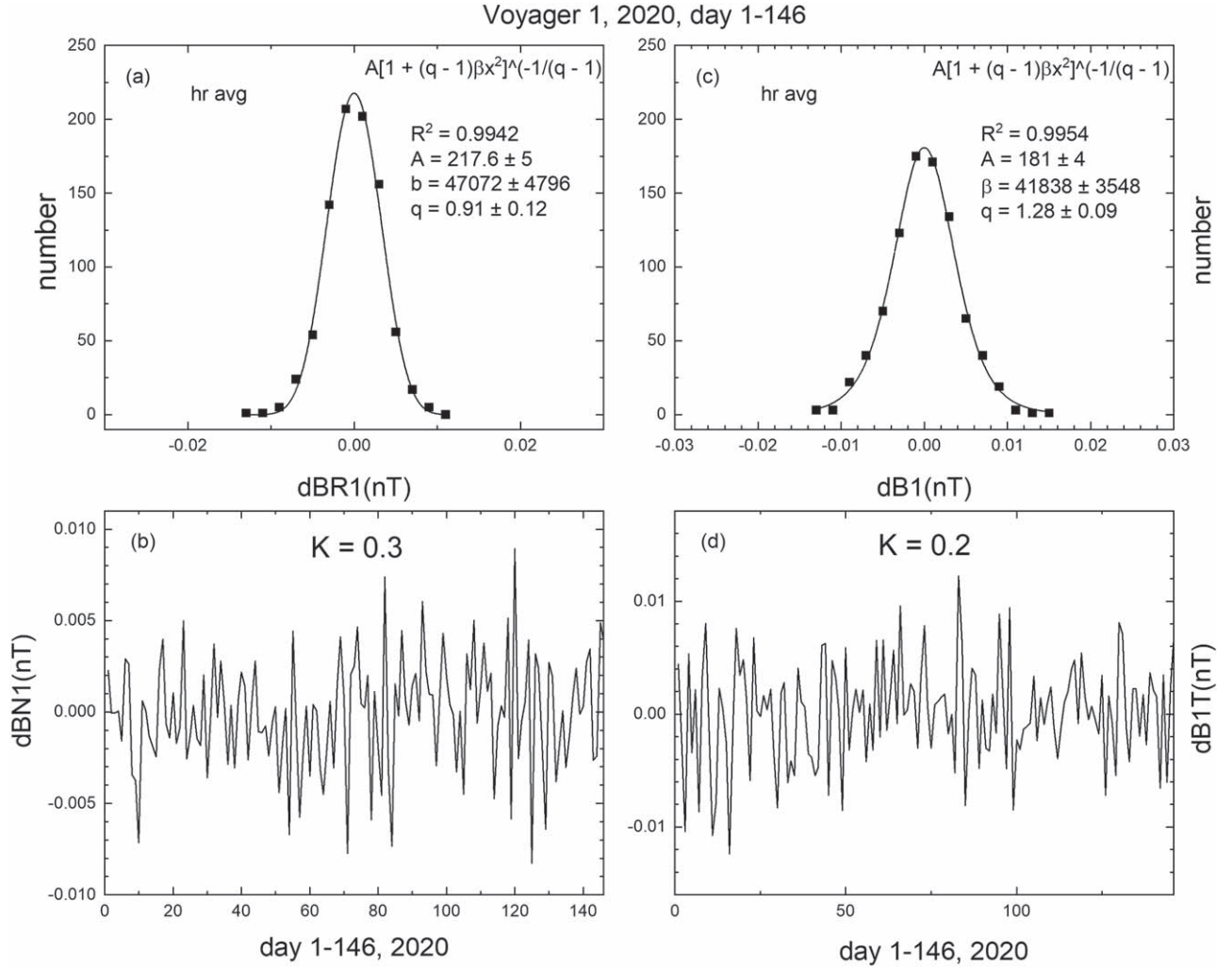


**Figure 3.** Intermittency in the dBN1 component and the dBT1 component in the magnetic hump, just following the arrival of the jump in  $B$  from day 147 to day 365, 2020.

parameter that measures the tails of the distribution, which quantitatively describe the intermittency, is the nonextensive parameter  $q = 1.3 \pm 0.1$ . Thus, the intermittency of  $dBN1(t)$ , which write as  $q$ -BN to be specific, is relatively small but significant, with an uncertainty of 8%.

The lower right panel in Figure 2(b) shows the time series of successive hourly increments of  $dBT1(t, \tau m) = dBT1(t + \tau m) - dBT1$ . Proceeding as above, we obtained a good fit of the distribution of increments  $dBT1(t, \tau m)$  using the  $q$ -distribution. In this case, the  $q$ -distribution also provides an excellent fit to the distribution of increments  $dBT1(t, \tau m)$  with  $R^2 = 0.992$ , which justifies our use of the  $q$ -distribution to describe observations of the increments of the field,  $dBT1(t)$ . The maximum amplitude of the distribution is given by  $A = 427 \pm 4$ . The parameter  $\beta$  measures the core distribution and is  $\beta = 40, 232 \pm 1,657$ . The parameter that measures the wings of the distribution, which describes the intermittency, is the nonextensive parameter,  $q$ -BT =  $1.33 \pm 0.05$ .

Now we turn to the observations of  $dBN1(t, \tau m)$  and  $dBT1(t, \tau m)$  in the magnetic hump just after crossing pf2 in the interval between about day 147 and 365, 2020, which is shown in Figure 3. The format of Figure 3 is the same as in Figure 2. In this

case, the time series of the measurements are plotted in panels (b) and (d) of Figure 3. This figure shows the first observations of the magnetic hump from day 147 to day 365, 2020, with its small random fluctuations in the increments accompanied by relatively large spikes in  $dBN1(t)$  and  $dBT1(t)$ . Prior to the magnetic hump, the values of  $q$ -BN and  $q$ -BT for the tails in the distribution of  $dBN1$  and  $dBT1$  from day one to day 146, were  $1.3 \pm 0.1$  and  $1.33 \pm 0.08$ , respectively. In the magnetic hump, just after crossing the jump pf2, the values of  $q$  for the tails in  $dBN1$  and  $dBT1$  were  $q$ -dBN1 =  $1.27 \pm 0.03$  and  $q$ -dBT1 =  $1.19 \pm 0.03$ , respectively. Thus, the value of  $q$  for the dBN component was  $q$ -dBN1 =  $1.3 \pm 0.1$  before the jump and  $1.27 \pm 0.03$  after the jump, indicating a change in  $q$ -dBN1 of 0.034. This change in  $q$ -dBN1 across the magnetic hump is within the uncertainties.

Similarly, the value of  $q$ -dBT1 was  $1.33 \pm 0.05$  before the jump pf2 and  $1.19 \pm 0.03$  after the jump indicating a change in  $q$ -dBT1 = 0.14, which is four times larger than the change in  $q$ -dBN1. Thus, there might have been a small change in  $q$ -dBN for dBN across the jump pf2, considering the uncertainties. The BR component is the smallest component of  $B$  and is directed radially away from the Sun, and it has the largest uncertainties, as discussed in the Appendix. The fluctuations in this

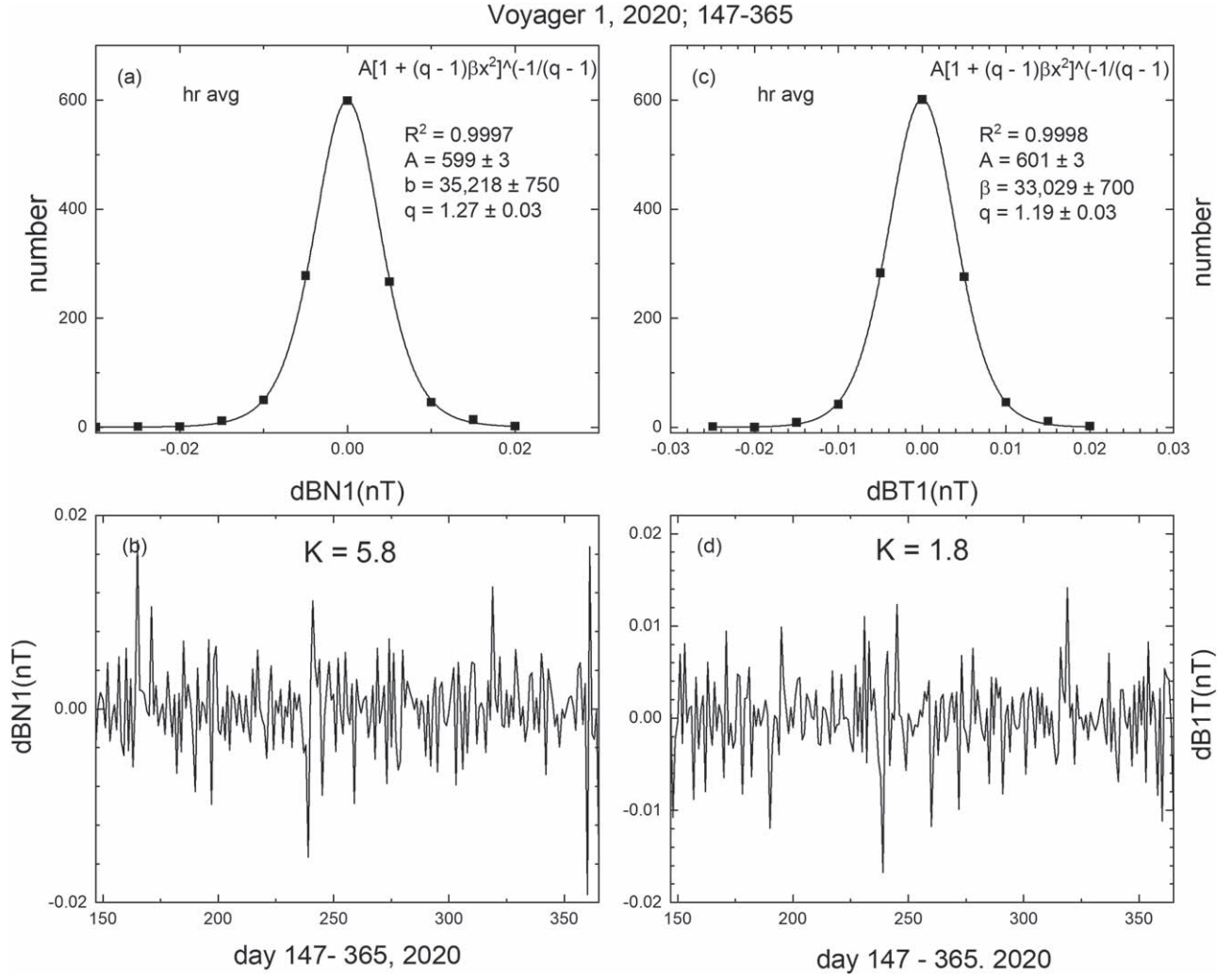


**Figure 4.** dBR1 and dB1 components of the increments of  $\mathbf{B}$  from day 1 to 146, 2020.

component from day 1 to 146 are shown in Figure 4. This component just ahead of the magnetic hump, from day 1 through day 146, is shown in Figure 4(b), which has the same ordinate scale as the previous components. The fluctuations are relatively weak because the component dBR1 itself is relatively small. There is no striking spikiness in the time series. The distribution function of dBR1 for the magnetic hump is shown by the observed points in Figure 4(b). The corresponding  $q$ -distribution is shown by the curves in Figure 5(a), which provides a very good fit to the observations of dBR1 following the jump in  $\mathbf{B}$ . The nonextensive index  $q = 0.91 \pm 0.012$  is consistent with no or very small fluctuations in dBR1 in the magnetic hump close to the jump pf2. The nonextensive index for dB1 is  $q = 1.28 \pm 0.09$ , which is larger because it includes all three components of  $\mathbf{B}$ .

Just after the arrival of the magnetic hump at V1, from day 147 to day 365, 2020, Figure 5(b) shows that the fluctuations in dBR1 are also very weak, as indicated by the small amplitude of the fluctuations. However, small spikes can be discerned, indicating the presence of weak intermittency. The distribution function of dBR1, shown in Figure 5, is described very accurately by the  $q$ -distribution. It is significant that although the amplitude of the fluctuations in dBR1 component is

relatively small, spikes, although relatively small, are present. Thus, the nonextensive parameter  $q = 1.27 \pm 0.03$  is significant even though the dBR1 component is relatively small.

Near the middle of the following year, 2021,  $\mathbf{B}$  in the magnetic hump reached a maximum, as shown in Figure 1. Figure 6 shows spikes in the dBN1 and dBT1 components, indicating intermittency for both the dBN1 and dBT1 components. The  $q$ -Gaussian distributions show significant intermittency, with  $q = 1.21 \pm 0.05$  for the dBN1 component and  $1.29 \pm 0.06$  for the dBT1 component. The fact that the observations so accurately describe the distribution of increments justifies the use of the  $q$ -Gaussian distribution.

The intermittency in the dBR1 and the dB1 components observed by Voyager 1 in the following year, 2021, are shown in Figure 7. The  $q$ -distribution describes the distributions of dBR1 and dB1 within the uncertainties, although there is some scatter about the  $q$ -distribution function. The parameter  $q = 1.2 \pm 0.2$  for dBR1 and the parameter  $q = 1.2 \pm 0.1$  for dB1 were obtained from the fits to the  $q$ -distribution for dBR1 and dB, respectively.

The intermittency observed by Voyager 1 during 2021 was weaker than that observed near the maximum of the magnetic hump during 2020, but the magnetic field strength still

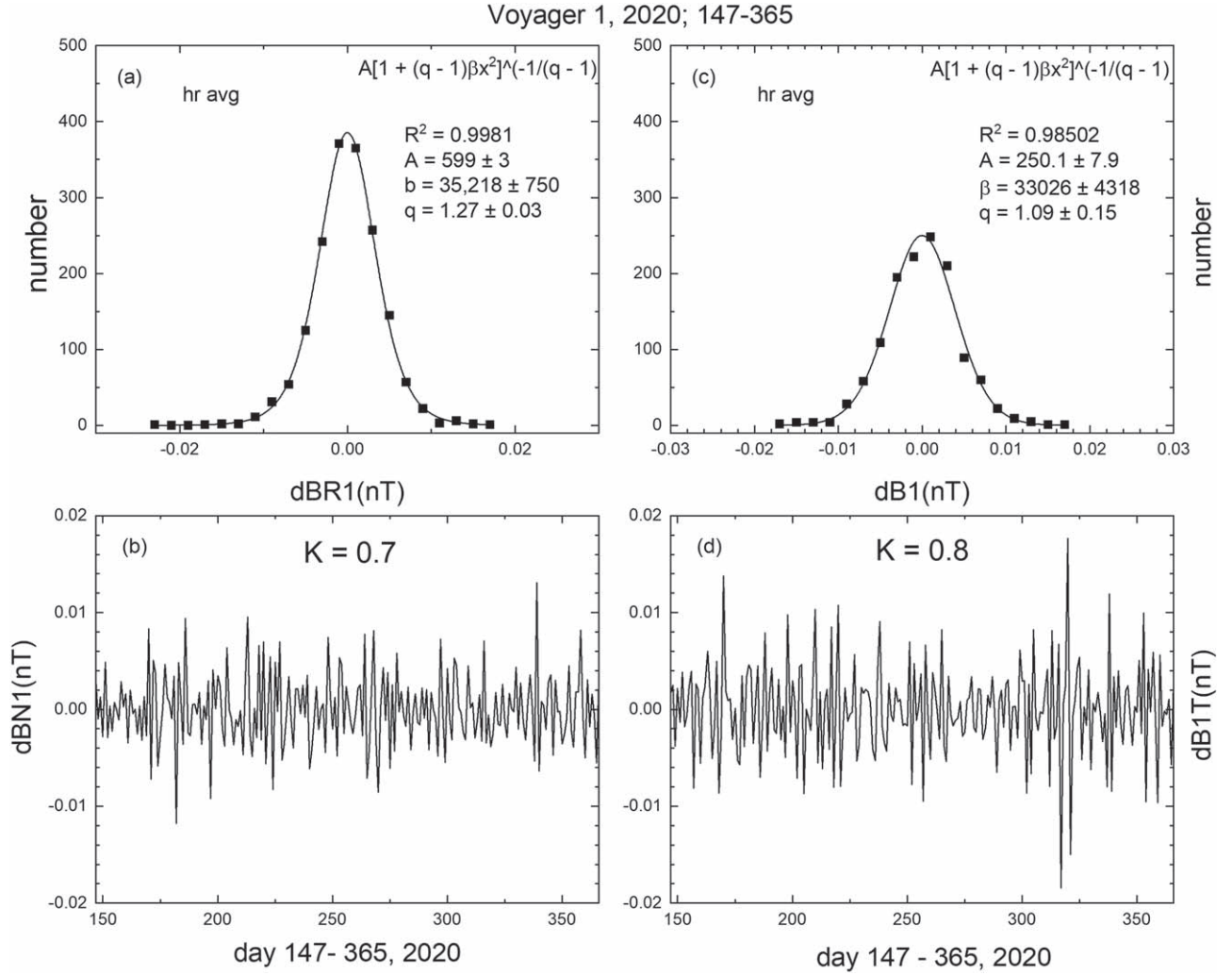


**Figure 5.** Intermittency in the dBR1 component and dB1 behind the magnetic hump.

remained higher than when Voyager 1 observed  $B$  behind of the jump pf2. Thus, Voyager 1 remained in the magnetic hump during 2021.

The intermittency observed by Voyager 1 during 2022 is shown in Figure 8. The distributions of the hourly increments of dBN1 and dB1 were  $q$ -distributions, with  $q$ -dBN1 =  $0.82 \pm 0.05$  and  $q$ -dB1 =  $1.043 \pm 0.002$ . The latter uncertainty is very small, perhaps coincidentally, but it is clear that  $q$ -BN1 and  $q$ -BT1 are close to 1. It has been shown that when  $q = 1$ , the  $q$ -distribution is a Gaussian distribution (Tirnakli & Borges 2016). Indeed, the important paper of Tirnakli and Borges provides a map from equilibrium Boltzman-Gibbs statistics to the Tsallis interpretation of an out-of-equilibrium state or, under certain circumstances, the indication of a different structure to be understood (see, e.g., Berdichevsky 2023). In this work, we share the views of Tsallis and show that during 2022, the  $q$ -distribution was a Gaussian distribution within the uncertainties. Since Voyager 1 was still observing magnetic fields stronger than those observed before the jump pf2, it was probably still observing the magnetic hump during 2022. In this case, there was very little or no intermittency in the part of the magnetic hump observed during 2022. This is the first time that Voyager 1 observed a Gaussian distribution of hourly increments in all three components of  $B$  in the interstellar medium.

Finally, Figure 9 shows the distribution functions and intermittency for dBR1 and dB1 observed by Voyager 1 during 2022. The time series and the lower panels show basically a noise signal without large spikes. The distribution function for dBR1 has  $q$ -dBR1 =  $1.02 \pm 0.08$ , consistent with the absence of intermittency in dBR in the magnetic hump during 2022. The distribution of dB1 during 2022 is also consistent with a Gaussian distribution with dB1 =  $0.84 \pm 0.09$ .

#### 4. Variations in the Intermittency of the Magnetic Field in the VLISM from 2016 through 2022

We now discuss the values of the parameters  $q$ -dB1 and  $q$ -dBN1 derived from the  $q$ -distribution for the increments dB1, and dBN1 discussed above in the VLISM, and compare them with the earlier interstellar observations of the distributions, as discussed by Burlaga et al. (2020a). We omit both the region near the heliopause in which mode conversion from its compressible to transverse waves was taking place and the regions in which shocks sh1 and sh2 were observed. In particular, we consider the intermittency of  $B$  in the VLISM as measured by  $q$  from 2016 through 2022. We recall that the interval from day 1, 2016, to day  $\sim 146$ , 2020, was representative of the typical intermittent magnetic fields in

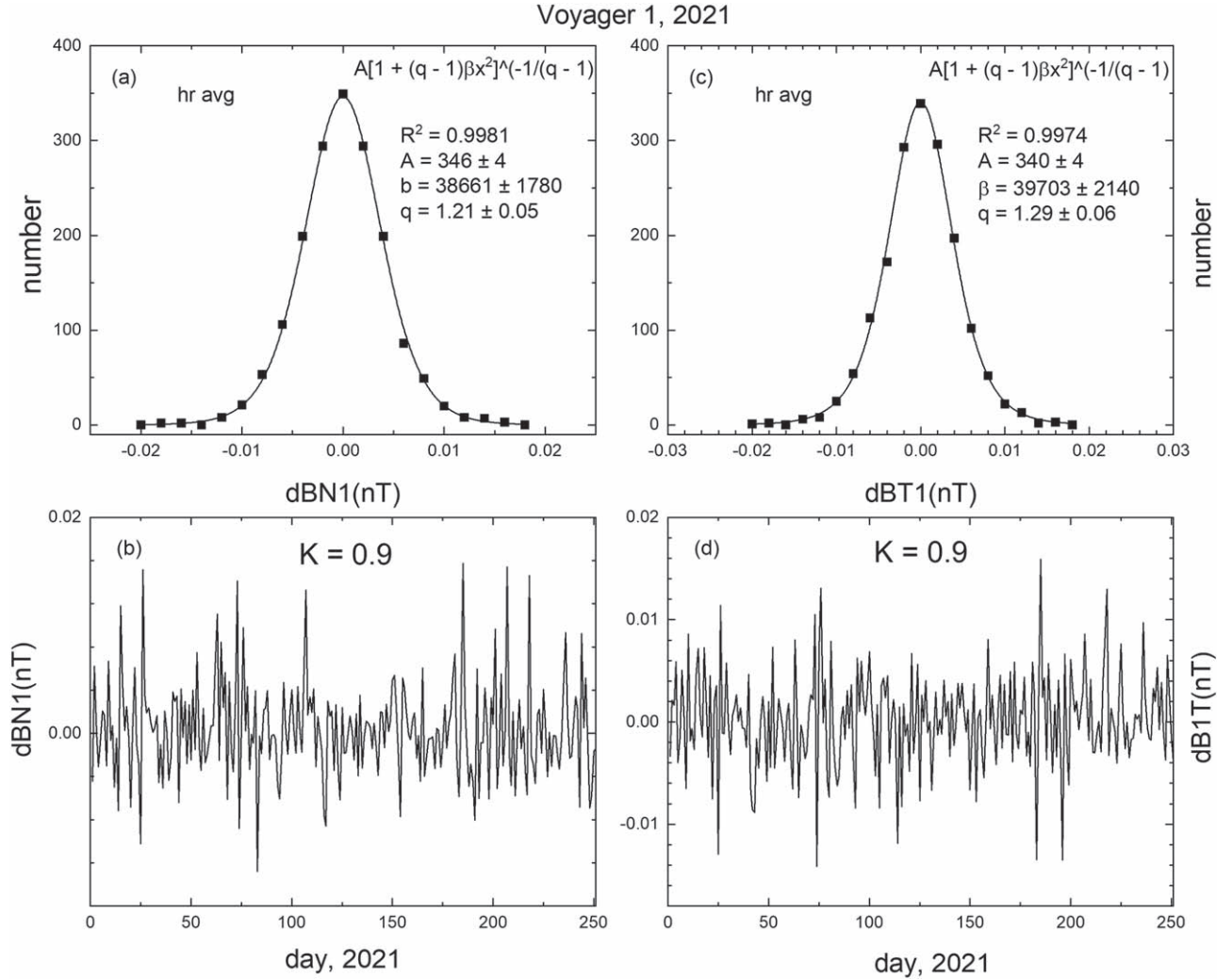


**Figure 6.** Intermittency in the dBN1 and dBT1 components of the magnetic field in 2021.

the VLISM, and the observations from day  $\sim 147$ , 2020, through 2022 revealed an unexpected magnetic hump with persistent strong magnetic fields following a jump pf2 in  $B$  measured by Voyager 1. Figure 10 shows the one-year averages of  $q$ -dBT1, and  $q$ -dBN1 for the distribution of hourly increments dBN1 (black squares) and dBT1 (red triangles) from 2016 through 2022, as well as for the radial component dBR (green triangles) for 2020 through 2022. We note that for clarity, the point at 2016.0 in Figure 10 refers to the entire year 2016, and likewise for 2017, 2018, 2019, 2020, 2021, and 2022. Similarly, the point at 2020 refers to the average value increments in the interval from day 1 to day 146, 2020, and the point at  $\sim 2020.5$  refers to the interval from 2020 day 147 to 2021.

Now we describe the temporal evolution of the intermittency of the increments of the  $\mathbf{B}$  components described by the parameters BT, BN, and BR and the corresponding  $q$ -Gaussian distribution functions from 2016 to 2023.0. The intermittency, indicated by the values of  $q$ -dBN, was larger in the predominantly transverse dBN1 component than the values of  $q$ -dBT1 in the compressible dBT1 component throughout the interval 2016 through 2020. Following a small decrease in  $q$ -dBN1 and  $q$ -dBT1 during 2016,  $q$  increased to a maximum in 2019, after which it decreased to near unity at the end of 2022. There was a dip in  $q$ -dBT following the maximum of

$q$ -dBT1 at the time of the jump in  $B$  at pf2 and the increase in the  $B$  strength behind it.

During 2022,  $q$ -dBR1 and  $q$ -dBT1 were equal to one within a one-sigma uncertainty, which means that the distribution was Gaussian for each of these components of  $\mathbf{B}$ . The  $q$ -dBN1 component was  $\sim 0.8$  nT. This is the only year in which Voyager 1 observed a Gaussian distribution for the increments of the three components of  $\mathbf{B}$  and unity (within the error bars) for the three values of  $q$ . This surprising result was observed even though the values of  $B$  had not returned to the pre-hump value, indicating that Voyager 1 was still moving through the magnetic hump.

## 5. Summary and Discussion

The primary objective of this paper is to compare the intermittency observed in the magnetic hump by Burlaga et al. (2022) from day  $\sim 147$ , 2020, to the end of 2022 with the intermittency observed earlier in the VLISM in the absence of the magnetic hump. In the earlier paper by Burlaga et al. (2023), it was shown that the distribution of consecutive hourly increments of the magnetic field components was the  $q$ -Gaussian distribution introduced by Tsallis (1988) in the context of nonequilibrium statistical mechanics. The



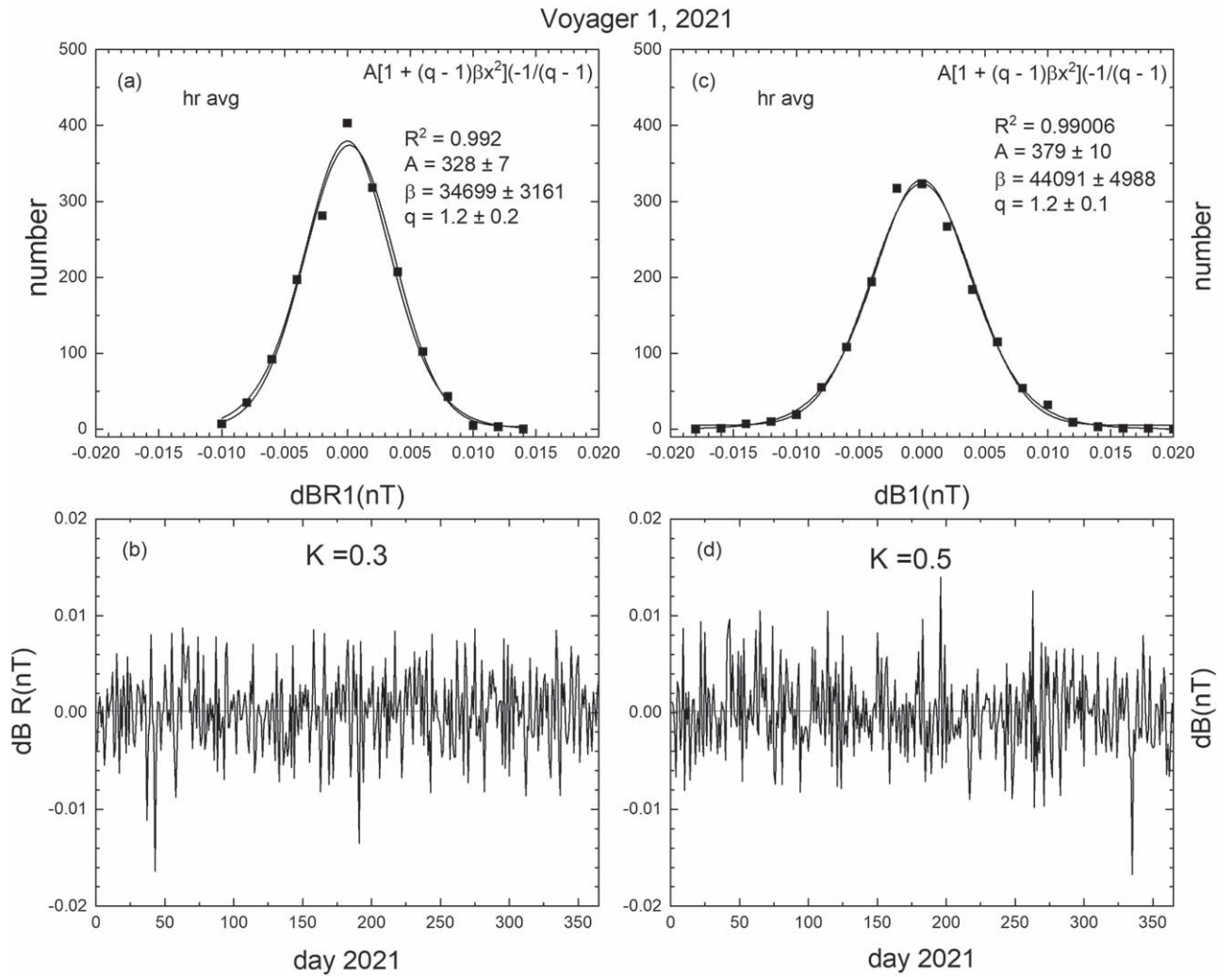


Figure 7. Intermittency in the dBR1 component and the dB1 magnitude of the magnetic field in 2021.

parameter  $q$  provides a definition of intermittency (a measure of the tail of the distribution) that is related to the distribution of increments of the observations of the components of the magnetic field.

We showed that the distribution of 1 hr increments of the BR, BT, and BN components of the magnetic field were accurately described by  $q$ -Gaussian distributions during the intervals from (a) 2020 DOY 1 to 2020/DOY 146, (b) 2020/DOY 147 to 2020/DOY 365, (c) from 2021/DOY 1 to 2021/DOY 365, and (d) 2022 DOY 1 to 2022 DOY 365. Previous observations in the VLISM by Burlaga et al. (2020b) also showed that  $q$ -Gaussian distributions of hourly increments of BN and dB1 were observed 2016, 2017, 2018, and 2019. There was little change in  $q$ -dB1 and  $q$ -dB1 before and after crossing the magnetic hump, although the uncertainties are significant.

We showed that the intermittency of BN and BT varies with time and/or distance from the Sun. The lowest values of  $q$ -dB1 and  $q$ -dB1 measured in the VLISM occurred in 2022, when Voyager 1 was still in the magnetic hump. In this case, the  $q$ -distributions of  $q$ -dBR1,  $q$ -dB1, and  $q$ -dBN1 observed during an interval of one year were Gaussian distributions, with  $q = 1$  within the uncertainties. This is the first evidence of Gaussian distributions of increments of components of  $\mathbf{B}$  in the

VLISM, indicating an absence of intermittency in 2022, within the uncertainties of the measurements.

As discussed by Burlaga et al. (2021) and shown in Figure 1, the arrival of the magnetic hump at V1 was associated with an abrupt increase in  $B$  and density. As Mostafavi et al. (2022) and others have suggested based on shock theory, it is likely that a jump such as this would propagate beyond Voyager 1 and steepen into a shock.

In fact, Fraternali et al. (2020) showed that the shock sh2 identified by Burlaga & Ness (2016) was accompanied by relatively strong intermittency. The passage time (thickness) of this jump was only slightly greater than that of shock sh2 in the VLISM discussed by Burlaga & Ness (2016). The magnetic field strength increased across the shock by  $B2/B1 = 1.13$ , and the density increased by  $N2/N1 = 1.1$ . The width of the laminar shock was 3.3 days, and its normal was  $16^\circ$  from the radial direction.

It is likely that jump pf2 will likewise steepen to a shock beyond the position of Voyager 1 and that intermittency would be associated with this shock, although we do not have observations to confirm this. It is likely that intermittency will be observed by Voyager 1 when shocks propagate to large distances from the Sun. Since the Sun is currently very active, Voyager 1 might observe shocks and intermittency approximately six years from now.

## Voyager 1, 2022

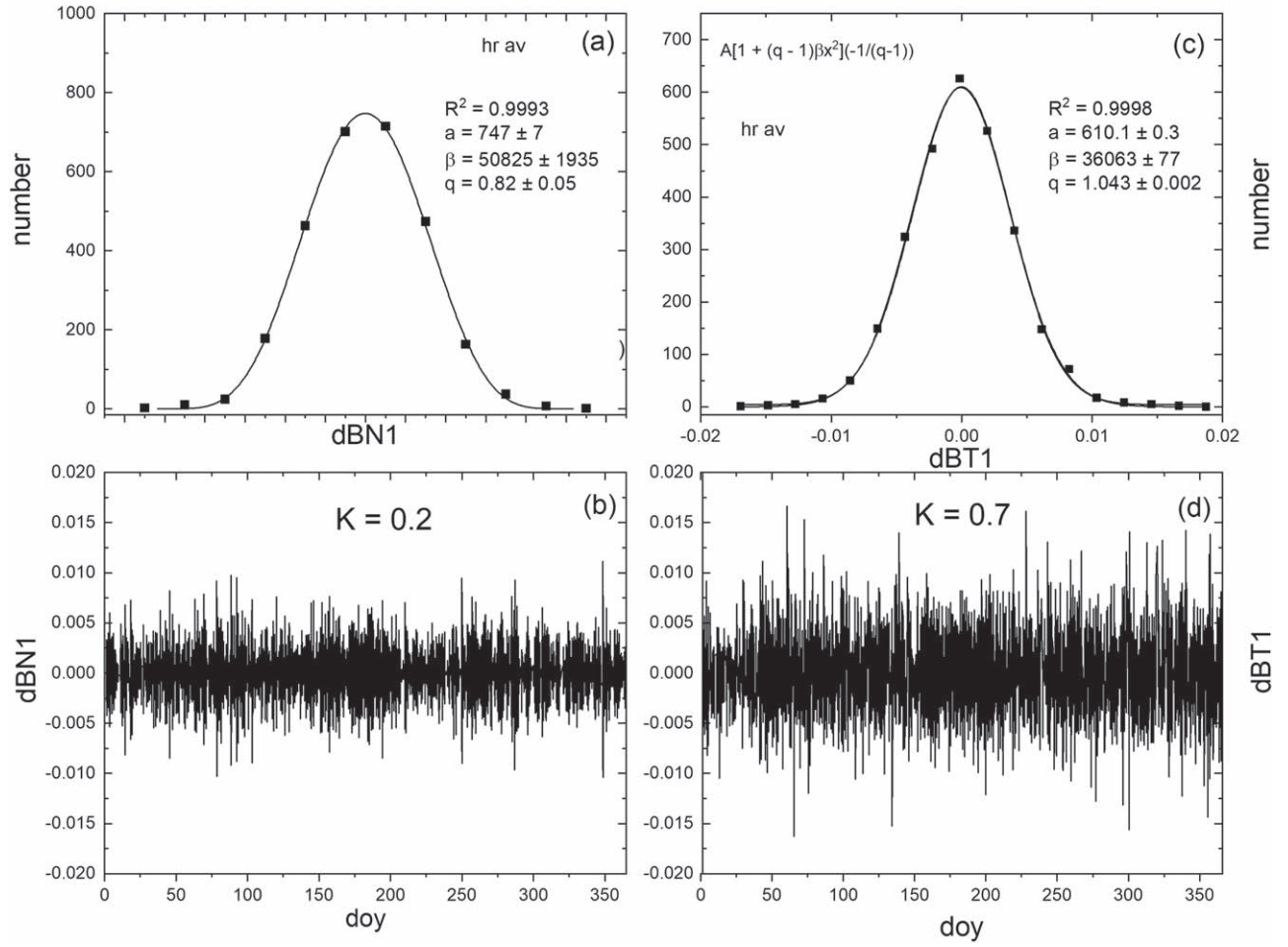
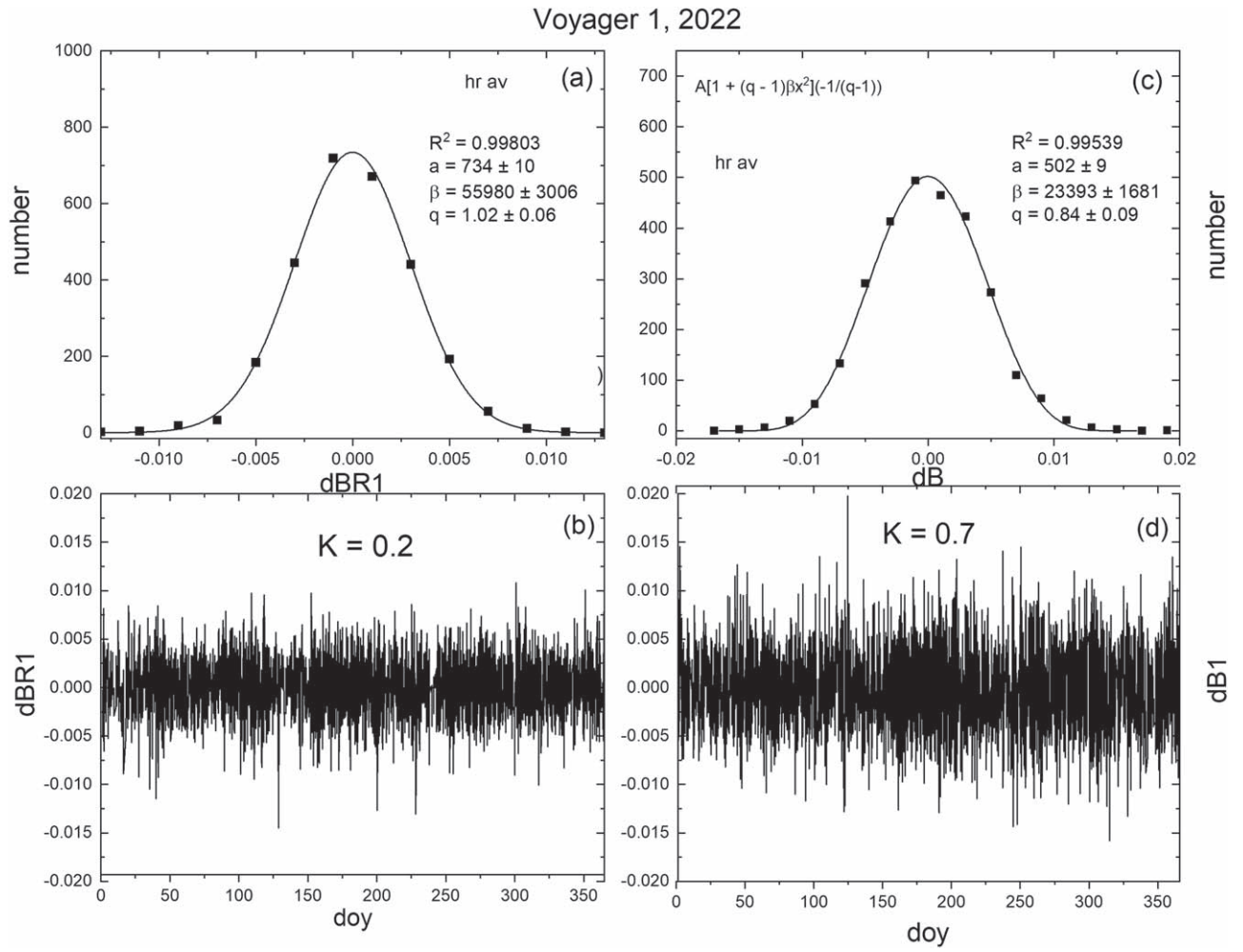
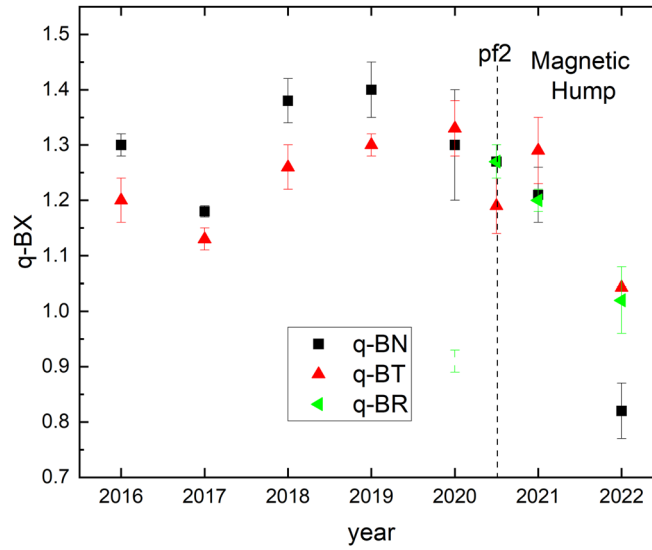


Figure 8. dBN1 and dBT1 components during 2022.



**Figure 9.** Observations of dBR1 and dB1 by Voyager 1 during 2022.



**Figure 10.**  $q$ -dBR,  $q$ -dBT, and  $q$ -dBN, the nonextensivity parameters describing the tails of the  $q$ -Gaussian distribution process of the increments of the components of  $B$ , plotted as a function of time as described by the distribution functions of the increments dBN1, dBT1, and dBR1 measured by Voyager 1 from 2016 through 2022.

## Appendix

Our discussion of intermittency includes intermittency in the BR component. Rankin et al. (2023) extrapolated the recent observations of the magnetic field theoretically and found that their theoretical model of the magnetic field with the observations of the BT and BN components agreed with the extrapolation of the Voyager observations of BT and BN. However, the observed BR component, which is weaker than the BT and BN components, decreased more rapidly with increasing distance from the Sun than the model of Rankin et al. predicted. They suggested that their theory is correct and the measured BR component is incorrect.

We show our estimate of the BR, which in the remainder of this paper discusses how the BZ PL component of the magnetic field observed by Voyager was computed from the radial component of the MAGCALs from day 181 to 365 inclusive, 2021. The

calibration method currently used is discussed in the document “Voyager Mission, Detailed processing of weak magnetic fields II —Update on the cleaning of Voyager magnetic field  $B$  with MAGCALs” by Daniel Benjamín Berdichevsky, College Park, Maryland, USA.

We start with the MAGCALs part of the sequential change of the sensor when functioning as illustrated by its effect on the data in the Figure 11. Small numbers on top of the sequence of a MAGCAL cycle of reversing the phase by  $180^\circ$  in the standing wave controlled by the vibration of monocrystal mode are shown in the example. The clean electromagnetic signal produced by the crystal has more than  $10^5$  oscillations per second. In Voyager, the analogical circuit that as its core includes the coil constitutes each one of the sensors of the magnetometer. We use the information of Figure 11 to evaluate the intensity of the component of the magnetic field along the radial direction from the Sun since Voyager 1 entered the

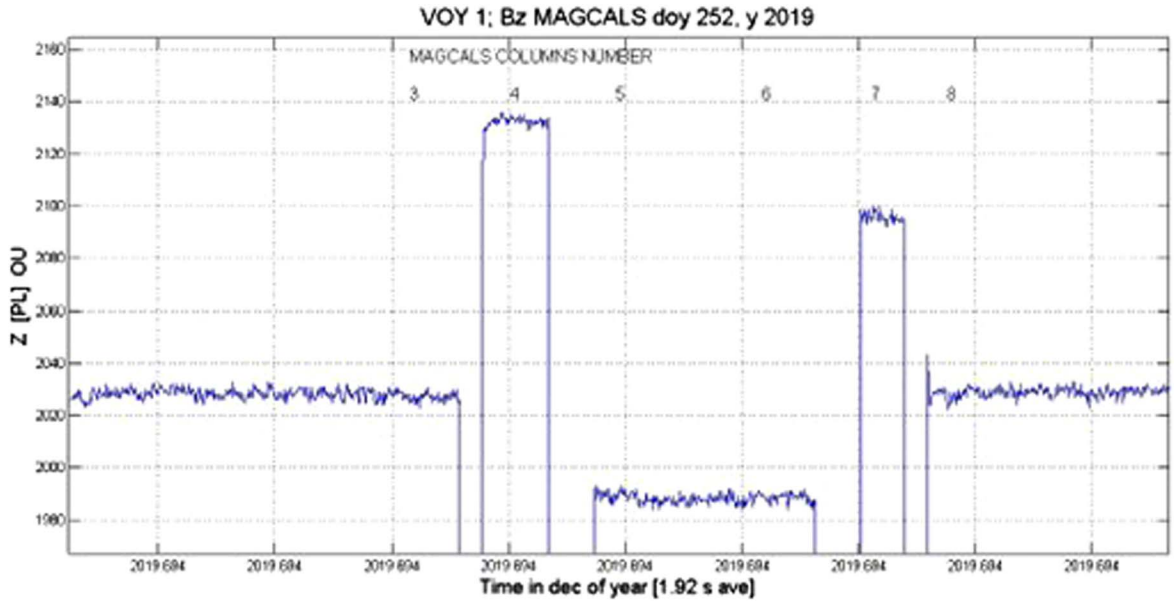


Figure 11.  $B$  component of MAGCAL on day 252, 2019.

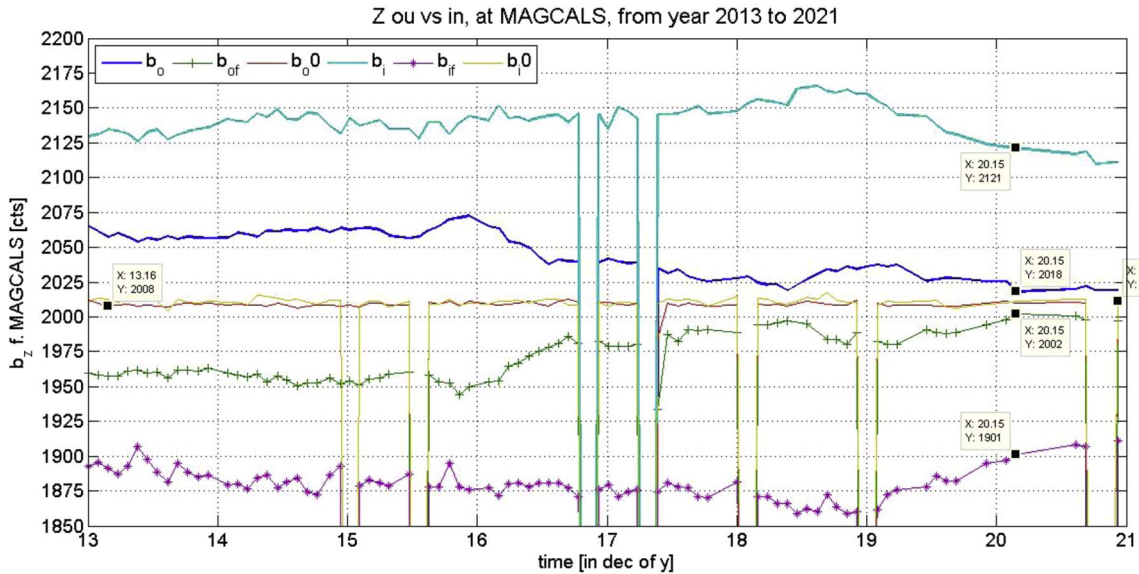
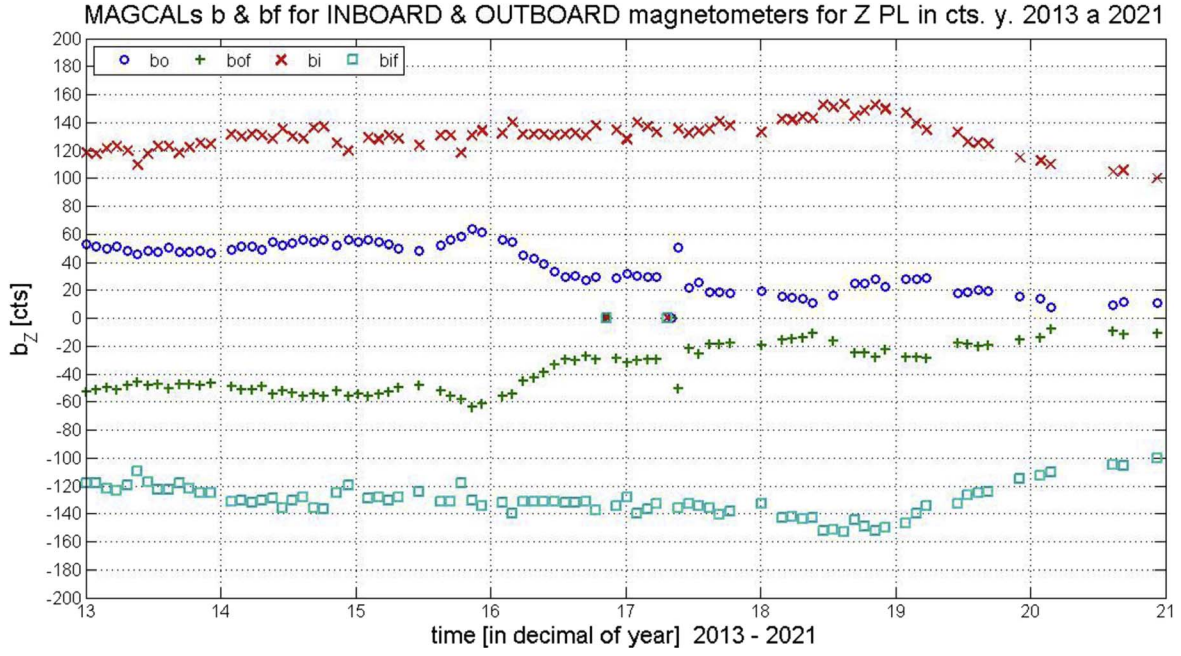
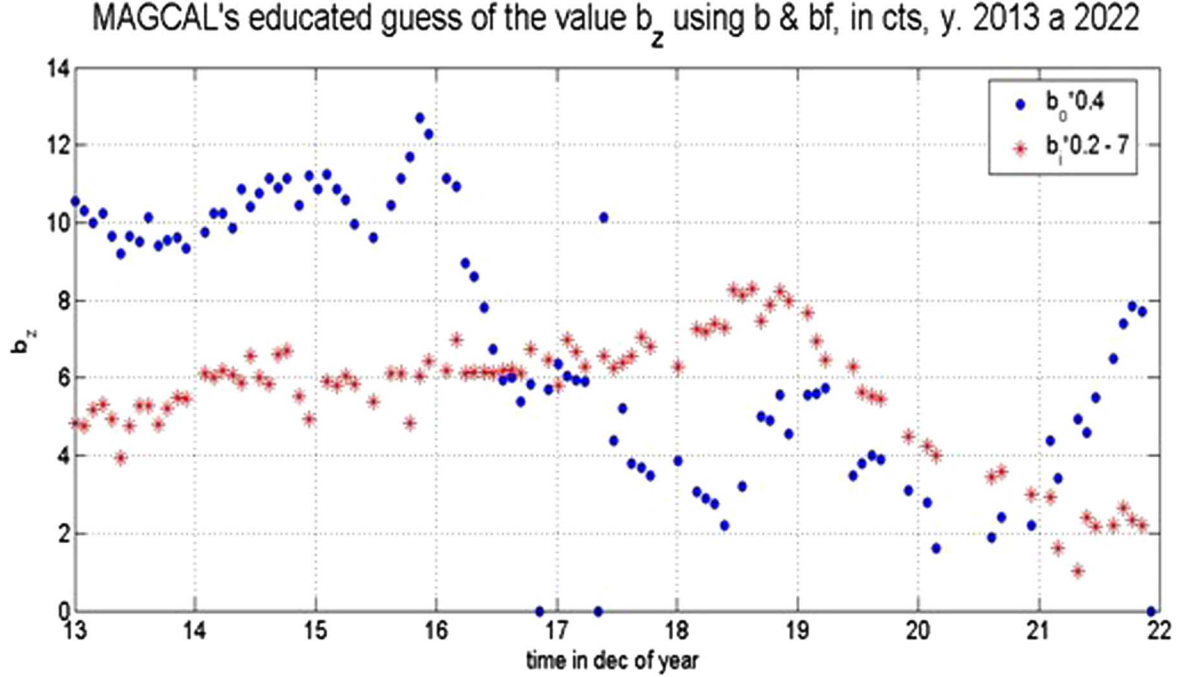


Figure 12. Evolution of the values  $b$  and  $b_f$  measured by the inboard and outboard magnetometer sensors during the MAGCALs from 2013 to 2021.





**Figure 13.** Intensities of  $b'_{IN}$  and  $b'_{OU}$ , which are subtracted by the absolute zeros  $b_{0IN}$  and  $b_{0OU}$  from the measured  $b_{IN}$  and  $b_{OU}$ , in counts. ‘bi,’ and ‘b0’ are the corresponding labels, filling the legend inset top left. One count is equal to 0.005 nT. The Z PL direction is toward to the Earth, which is approximately radial from the Sun because the location of the two Voyager spacecraft is well beyond the distance between the Sun and the Earth. This radial direction pointing toward the Sun is Z PL oriented inward in a right-handed coordinate. Hence the plot of the quantities in Equation (2a) and (2b) once the  $b_{0IN}$  and  $b_{0OU}$  are subtracted are displayed.



**Figure 14.**  $b_z$  vs. time in decimal years.

VLISM (sunward being positive along the Z-direction of the right-handed payload (PL) axes of the Voyager magnetometer used for calibration purposes).

The information contained in Figure 11 labeled “b” (the mean of the values c3 and c8 of the steps in Figure 11) and “bf” (the mean of the values c5 and c6 of the steps in Figure 11) for several years is used to estimate the intensity of the component of the magnetic field along the Z-PL direction

by identifying the location of the zeros. Only a linear combination of b and bf is needed for the calculations. Figure 12 shows the evolution of this specific part of the collected MAGCALs b and bf for an extended period of time for the Voyager 1 spacecraft. We take advantage of the presence of two Z PL sensors. One of these Z PL sensors is part of the outboard (OU) magnetometer and the other of the inboard (IN) magnetometer.

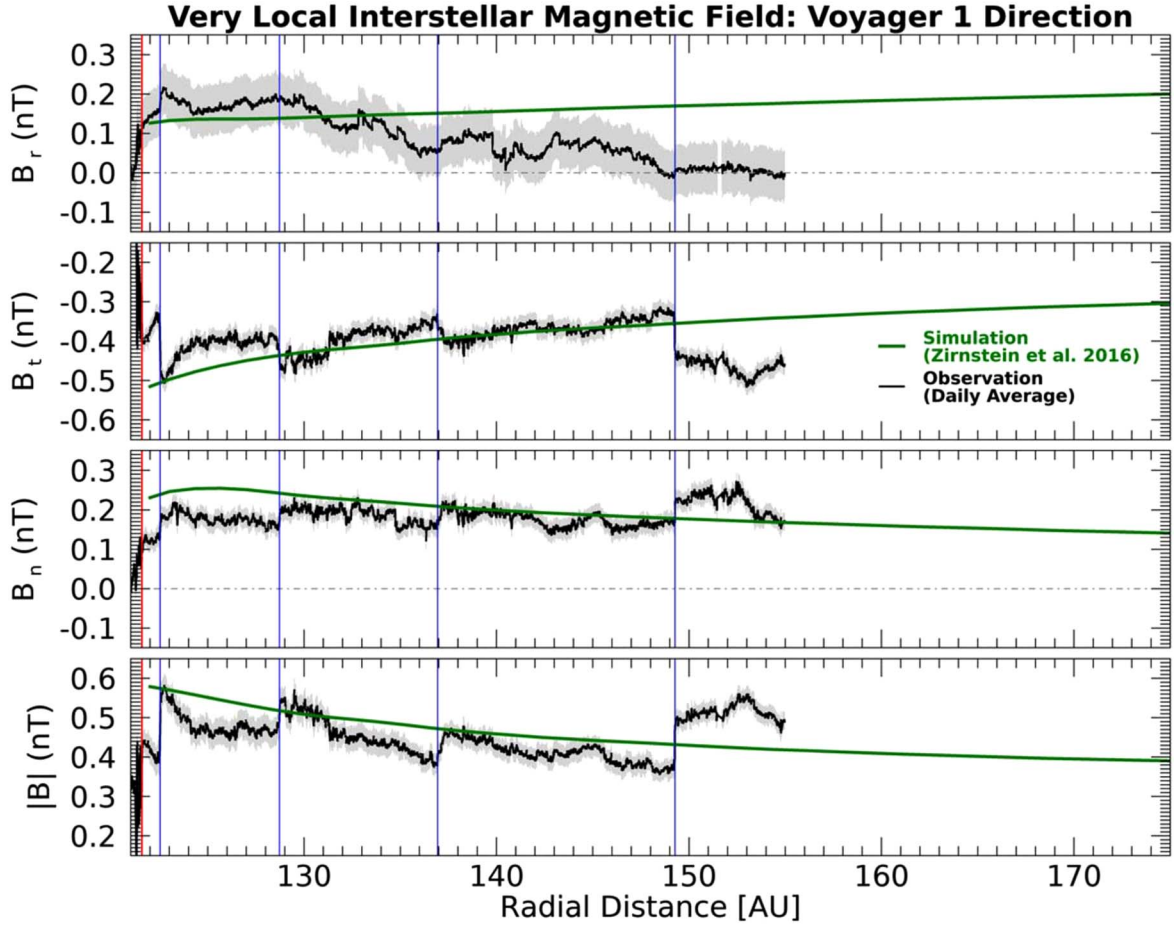


Figure 15. Magnetic field components in RTN coordinates and total strength from 120 to 175 au from Rankin et al. (2023), ApJ, 945, L31.

We use the information of Figure 11 to evaluate the intensity of the component of the magnetic field along the radial direction from the Sun since Voyager 1 entered the VLISM (sunward being positive along the Z-direction of the right-handed payload (PL) axes of the Voyager magnetometer used for calibration purposes).

Then we consider the steady line obtained by calculating for IN and OU the value

$$b_0 = \frac{1}{2}(b + bf), \quad (\text{A1})$$

which indicates the location of the absolute zero of the instruments and which we use as a reference level in Figure 13. The observed values are referred to this “absolute zero”.

Then we follow the instructions from Berdichevsky (2015) to evaluate the constraints on the intensity of the component of the magnetic field along Z PL. In this case, we consider the relations

$$b_{\text{IN}} = b_{\text{INSC}} + bm \quad (\text{A2a})$$

and

$$b_{\text{OU}} = b_{\text{OUSC}} + bm \quad (\text{A2b})$$

as well as the zeros for  $b_{0\text{IN}} = (b_{\text{IN}} + bf_{\text{IN}})/2$  and  $b_{0\text{OU}} = (b_{\text{OU}} + bf_{\text{OU}})/2$ , which coincide in the case of the Z PL sensors of the IN and OU magnetometers. Hence, the plot of the quantities in Equations (A2a) and (A2b) once the  $b_{0\text{IN}}$  and  $b_{0\text{OU}}$  are subtracted are displayed.

This sets a constraint on the value of  $bm$ , considering the fact that Equations (A2a) and (A2b) along Z PL, the intensity of the field of the medium, has to satisfy

$$bm < b_{\text{OU}}, \quad (\text{A3a})$$

where

$$b_{\text{OU}} < b_{\text{IN}}. \quad (\text{A3b})$$

In a previous discussion of the problem considered here, we identified that by a change of coordinates, the value of  $bm$  would be located somewhere along a line of known slope,

$$m = (b_{\text{IN}} + b_{\text{OU}})/(b_{\text{IN}} - b_{\text{OU}}). \quad (\text{A4})$$

Using the current understanding of the magnetic field at the latest large compression, the magnetic field intensity along Z PL (approximately radial from the Sun) was lower than 4 or 5 counts. In consequence, we aim for the estimate of the  $B$ -field to determine a value for  $bm$  close to constant and small. We estimate that the Z-component of the magnetic field is within  $4 \pm 4$  counts ( $0.02 \pm 0.02$  nT), as illustrated in Figure 14. We use this estimate to complete the calibration for the last half of 2021.

Figure 14 illustrates the estimation of the values, and furthermore, their error is indicated below in the text. From

lessons learned from adjustments for the  $X$  and  $Y$  PL directions,

$$b_i = b_i Z(\text{abs0}) - 1/6(Z_{\text{IN}8\text{column}} - Z_{\text{IN}7\text{column}}) + 2/27(Z_{\text{IN}4\text{column}} - Z_{\text{IN}5\text{column}}) - 2\text{Cts}, \quad (\text{A5a})$$

$$b_o = b_o Z(\text{abs0}) - 1/6(Z_{\text{OU}8\text{column}} - Z_{\text{OU}7\text{column}}) + (1/4)^2(cZ_{\text{OU}4\text{column}} - cZ_{\text{OU}5\text{column}}) + 25\text{Cts}, \quad (\text{A5b})$$

where we loosely follow the notation in a newer document in its draft version on the adjustment for the determination of the zeros empirically found with the MAGCALs and currently used for  $X$  and  $Y$  PL directions. In the end, Figure 14 shows reasonable values with the improved MACALs estimates of  $bZ_{\text{IN}}^1$  and  $bZ_{\text{OU}}^1$ ,

$$bZ_{\text{IN}}^1 = 0.2b_i - 7\text{Cts}, \text{ and} \quad (\text{A6a})$$


$$bZ_{\text{OU}}^1 = 0.4b_o. \quad (\text{A6b})$$

The top panel of Figure 15 shows the BR component of  $\mathbf{B}$  measured by Voyager 1 as a function of distance from the Sun. BR decreases significantly with increasing distance from the Sun, whereas the theoretical model of Rankin et al. (2023) predicts an increase with distance. We estimate that the  $Z$ -component of the magnetic field is  $4 \pm 4$  counts ( $0.02 \text{ nT} \pm 0.02 \text{ nT}$ ) near the magnetic hump, as illustrated in Figure 15.

We use a technique (the MAGCAL flip) that describes the location of zeros through a linear combination of the stages in the changes presented in Figure 11. The technique applies to all magnetic field sensors (six in total in Voyager 1; three are for the outboard magnetometer, and another three are for the inboard magnetometer). This calibration is equivalent to the use of MAGROLs. It gives strong support for the use of linear combinations of the observation of the flip part of the magnetic field at MAGCALs. This case is optimal, within the uncertainties of each sensor, to locate the estimated zeros. We have been doing this for the radial direction (BR) for at least for the last 20 years, since the SC moved beyond the end of the heliosheath.

However, we show in Figure 14 a straightforward estimate at MAGCALs of the intensity  $b$  at the IN and OU sensors along  $Z$  PL as is indicated by the final Equations (A6a) and (A6b) consistent with the labeling in Figure 14. For the specific dependence on the MAGCAL flip stages in Figure 11, we refer to the relation of Equation (6) with the explicit expressions in Equations (A5a) and (A5b).

## ORCID iDs

L. F. Burlaga  <https://orcid.org/0000-0002-5569-1553>  
D. B. Berdichevsky  <https://orcid.org/0000-0001-9357-7973>  
L. K. Jian  <https://orcid.org/0000-0002-6849-5527>  
J. Park  <https://orcid.org/0000-0002-8989-4631>  
A. Szabo  <https://orcid.org/0000-0003-3255-9071>

## References

- Behannon, K. W., Acuna, M. H., & Burlaga, L. F. 1977, *Space Sci. Rev.*, **21**, 235
- Berdichevsky, D. B. 2009, Voyager Mission, Detailed Processing of Weak Magnetic Fields; I - Constraints to the Uncertainties of the Calibrated Magnetic Field Signal in the Voyager Missions, NASA, [https://spdf.gsfc.nasa.gov/pub/data/voyager/documents/vgvmag\\_website/Berdichevsky-VOY\\_sensor\\_opu090518.pdf](https://spdf.gsfc.nasa.gov/pub/data/voyager/documents/vgvmag_website/Berdichevsky-VOY_sensor_opu090518.pdf)
- Berdichevsky, D. B. 2015, Voyager Mission, Detailed processing of weak magnetic fields; II - Update on the cleaning of Voyager magnetic field density B with MAGCALs, version 11/7/2015, NASA, [https://spdf.gsfc.nasa.gov/pub/data/voyager/documents/vgvmag\\_website/20151017BzPLestimates\\_wMAGCAL.pdf](https://spdf.gsfc.nasa.gov/pub/data/voyager/documents/vgvmag_website/20151017BzPLestimates_wMAGCAL.pdf)
- Berdichevsky, D. B. 2023, Modern Permanent Magnets - Fundamental and Application, doi:10.5772/intechopen.112362
- Burlaga, L. F., Kurth, W. S., & Gurnett, D. A. 2021, *ApJ*, **911**, 61
- Burlaga, L. F., & Ness, N. F. 2016, *ApJ*, **829**, 134
- Burlaga, L. F., Ness, N. F., Berdichevsky, D. B., et al. 2020a, *AJ*, **160**, 40
- Burlaga, L. F., Ness, N. F., Berdichevsky, D. B., et al. 2020b, *ApJL*, **901**, L2
- Burlaga, L. F., Ness, N. F., & Berdichevsky, D. B. 2022, *ApJ*, **932**, 59
- Burlaga, L. F., Ness, N. F., Gurnett, D. A., & Kurth, W. S. 2013, *ApJL*, **778**, L3
- Burlaga, L. F., Porgorelov, N., & Jian, L. K. 2023, *ApJ*, **953**, 135
- Burlaga, L. F., Viñas, A., Ness, N. F., & Acuña, M. H. 2006, *ApJL*, **644**, L83
- Fraternali, F., Porgorelov, N., & Burlaga, L. F. 2020, *ApJL*, **897**, L28
- Frisch, U. 1995, *Turbulence: The Legacy of A.N. Kolmogorov* (Cambridge: Cambridge Univ. Press)
- Gurnett, D. A., Kurth, W. S., Burlaga, L. F., & Ness, N. F. 2013, *Sci*, **341**, 1489
- Holzer, T. E. 1989, *ARA&A*, **27**, 199
- Kleimann, J. D., Fraternali, G. A., Heerikhuisen, J., et al. 2022, *SSRv*, **218**, 36
- Krimigis, S. M., Decker, R. B., Roelof, E. C., et al. 2013, *Sci*, **341**, 144
- Livadiotis, McComas, D. J., Dayeh, M. A., Funsten, H. O., & Schwadron, N. A. 2011, *ApJ*, **734**, 1
- Mostafavi, P., Burlaga, L. F., Cairns, I. H., et al. 2022, *SSRv*, **218**, 27
- Parker, E. N. 1963, *Interplanetary Dynamical Processes* (New York: Wiley)
- Pogorelov, N. V., Heerikhuisen, J., & Roytershteyn, V. 2017, *ApJ*, **845**, 9
- Rankin, J. S., McComas, D. J., Zirnstein, E. J., Burlaga, L. F., & Heerikhuisen, J. 2023, *ApJL*, **945**, L31
- Sorriso-Valvo, L., Carbone, V. V., Consolino, G., & Bruno, R. 1999, *GeoRL*, **26**, 1801
- Stone, E. C., Cummings, A. C., & McDonald, F. B. 2013, *Sci*, **341**, 150
- Timakli, U., & Borges, E. 2016, *NatSR*, **6**, 23644
- Tsallis, C. 1988, *JSP*, **52**, 479
- Tsallis, C. 2004, *PhyA*, **340**, 1
- Zank, G. P. 2015, *ARA&A*, **53**, 449